Mathematics and Mechanics of Solids

http://mms.sagepub.com

The Size Effect of Thin Films on the Peierls Stress of Edge Dislocations

Chin-Long Lee and Shaofan Li

Mathematics and Mechanics of Solids 2008; 13; 316
DOI: 10.1177/1081286507086904

The online version of this article can be found at:
http://mms.sagepub.com/cgi/content/abstract/13/3-4/316

Published by:
SAGE
http://www.sagepublications.com

The Size Effect of Thin Films on the Peierls Stress of Edge Dislocations

CHIN-LONG LEE
SHAOFAN LI
Department of Civil and Environmental Engineering, University of California, Berkeley, CA 94720, USA

Abstract: In this paper, we have developed a half-space Peierls–Nabarro (HSPN) model to evaluate dislocation mobility on material surface. The free-surface induced size effect on the mobility of an edge dislocation in thin films is investigated by using the model. The thickness of the thin layer between the dislocation and the free surface significantly influences the mobility of the dislocation. The Peierls stress of the edge dislocation in a thin film may be expressed as a function of the thickness of the thin film. A closed-form solution is obtained for the scaling factor, defined as the ratio of the modified Peierls stress to the conventional one in bulk materials, which allows for the characterization of the size (depth) effect on the Peierls stress of the edge dislocation in the half-space. Depending on the core size of the dislocation, the Peierls stress of a surface edge dislocation is about 5% to 25% less than that found in bulk materials.

Key Words: Dislocations, lattice friction, Peierls–Nabarro model, scaling law, size effects

1. INTRODUCTION

Size effects of thin films on both electronic and mechanical properties of thin films have been a major concern in the fabrication of high quality ultra-thin film for either integrated circuits and devices of micro-electronic-mechanical systems (MEMS) or nano-electronic-mechanical systems (NEMS), e.g. [1–3]. In particular, the free-surface induced size effects on surface or near-surface dislocations have been an unresolved issue in material science and engineering, especially for nano-scale materials [4]. This study addresses the issue of the size effect of thin films on dislocation mobility, which is the crucial measure of the quality of epitaxial thin films. In principle, atomistic simulations can provide a realistic estimate of the lattice friction of a dislocation in a bulk material as well as for surface dislocations. However, the simulations based on first principles seldom provide analytical solutions and hence are not sufficient for providing general guidelines.

The first analytical formula of the lattice friction is given by Peierls and Nabarro [5, 6] using a continuum model combined with the atomic description of the dislocation core. In their model, denoted as the PN model in this paper, the single dislocation is replaced with a

Mathematics and Mechanics of Solids **13:** 316–335, 2008 DOI: 10.1177/1081286507086904

Los Angeles, London, New Delhi and Singapore

distributed dislocation such that the same Burgers vector can be recovered after the latter is integrated over the whole x-axis. This model, as noted in [7], further assumes that

(i) the traction-displacement relation obeys the sinusoidal force law inside the glide plane;
(ii) the material remains elastic outside this glide plane;
(iii) the temperature effect and thermal activation are neglected; and
(iv) the translation of the dislocation is rigid so that there is no change of the geometric core structure in the process.

Notwithstanding the above assumptions, the Peierls stress obtained from the PN model still provides a good estimation of the maximum lattice friction when the dislocation moves along the glide plane. However, their analytical formula, which is expressed in terms of summation of a series, is only valid for wide dislocations if the higher order terms are ignored. A simpler yet rigorous expression of this formula was later derived by [8] such that the obtained Peierls stress is valid for all sizes of the dislocation.

Since the PN model is an approximate model, it often tends to be inaccurate in predicting dislocation mobility. More accurate approaches such as ab initio methods based simulations that can accurately predict the so-called generalized stacking fault energy (gsf or γ energy), e.g. [9], are receiving more and more attentions. Nevertheless, many recent works still attempt to improve the PN model by accounting for arbitrary angles of Burgers vector [10–12], deriving the Peierls stress from the variational approach [13], obtaining the gsf energy for given materials [14], studying the effects of the dislocation core structure on the Peierls energy [15, 16], and correcting the counting schemes in summing the misfit energy density for the total misfit energy [17–19]. These works have significantly improved the applicability of the PN model to general crystal structures. The historical developments and limitations of this model have been documented in detail [20, 21].

Most improvements on the PN model are still limited to the dislocations in bulk materials. The boundary effect on the Peierls stress has not been discussed in the above mentioned studies. This shortcoming renders the PN model ineffective for dislocations in thin film structures that have a traction-free surface boundary.

Recently, the present authors proposed a half-space Peierls–Nabarro (HSPN) model to account for the traction-free surface boundary for a screw dislocation [7]. The basic hypothesis of the new model is that *the lattice friction or the mobility of a dislocation changes when the dislocation moves towards the traction-free surface. The reason why image stress is pulling dislocations out the bulk is not because of the Newtonian force due to image dislocation acting the particle where the real dislocation is moving through, but rather the change of the critical value of the configurational force, or, more precisely, the Peach-Koehler force acting on the defect—the very dislocation. And this critical value is the Peierls–Nabarro force—a measure of the lattice friction.*

The half-space PN model developed in [7] improves upon the PN model and uses a distributed image dislocation to remove the traction on the free surface. In addition to the assumptions listed above for the PN model, the HSPN model further assumes that

(i) the Burgers vector distribution can be viewed as an eigen-strain that remains self-contained regardless of the existence of the free surface; and

(ii) the formulas for the misfit energy and the resulting Peierls stress should be modified according to the true stress, which, other than the stress caused by the dislocation itself, also includes the stress due to the free surface at the glide plane.

The second assumption implies that the boundary stress due to the free surface interacts with the dislocation. With the two assumptions listed above, the HSPN model is feasible for analyzing the lattice friction of the dislocation in thin films and is therefore believed to be more attractive than the PN model.

The HSPN model leads to the development of the scaling factors between the HSPN and the PN models for both misfit energy and Peierls stress. Note that these factors were named as *amplification factors* in the previous study [7]. Since these factors do not exceed 1, they maybe better named as *scaling factors*, which are used in this paper. The factors with values less than 1 correspond to reductions in the misfit energy and the Peierls stress. There has been a speculation that the mobility near the free surface should be lower than that in the bulk material. This speculation has finally been confirmed quantitatively in [7]. In addition, these scaling factors provide the scaling ratios and an insight of the size effect (the depth of the dislocation) on both misfit energy and Peierls stress for different depths of the screw dislocation in a half-space. The authors also showed that the surface screw dislocation will not have zero but about 85% of the Peierls stress in bulk materials. The reduction in the Peierls stress is found to be not much because this Peierls stress is for dislocation moving in the glide plane rather than in the climb plane (the plane that is perpendicular to the free surface), where the latter is believed to have a higher reduction.

In this paper we will extend the HSPN model developed in [7] to the case of an edge dislocation. The idea for constructing the HSPN model for the edge dislocation is however different from that advanced in [7] for the screw dislocation, which will be illustrated further in the paper.

2. HALF-SPACE PEIERLS–NABARRO (HSPN) MODEL

In the following, we will derive the HSPN model by following similar steps to those in the previous study [7, 22].

2.1. Burgers Vector Distribution

Consider an edge dislocation with a Burgers vector, $\mathbf{b} = b\mathbf{e}_x$, in the direction [100] of a crystal, and embedded at depth h in a half-space (see Figure 1). The elastic shear modulus of the material of the half-space is denoted by μ.

Before the formation of the edge dislocation, the half-space ($-\infty \leq y \leq h$) shown in Figure 1 can be split into two parts: the top layer ($0 \leq y \leq h$) and the bottom half-space ($y \leq 0$) separated by a distance d (see Figure 2). The disregistry between the top layer and the bottom half-space at $y = 0$ is

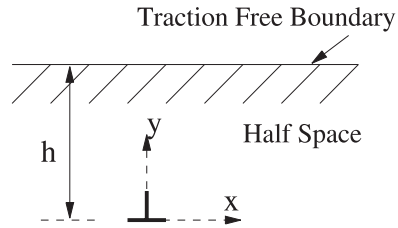

Figure 1. An edge dislocation embedded with depth h in a half-space.

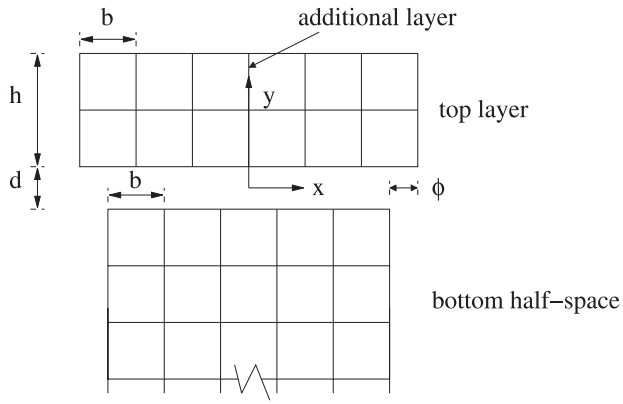

Figure 2. Half-space split into top layer ($0 \le y \le h$) and bottom half-space ($-\infty \le y \le 0$) separated by a distance d.

$$\phi_x^0(x) = \begin{cases} \dfrac{b}{2} & \text{if} \quad x > 0 \\ -\dfrac{b}{2} & \text{if} \quad x < 0 \end{cases} = \pm\frac{b}{2}. \tag{1}$$

For the "±" sign in the above equation, the "+" sign here is used if $x > 0$ and the "−" sign here is used if otherwise.

After these two bodies join together with a cohesive layer (non-Hookean slab) with thickness d in the middle ($-d/2 \le y \le d/2$) to form a new half-space with the edge dislocation as shown in Figure 3, the disregistry at $y = 0$ becomes

$$\phi_x(x) = \pm\frac{b}{2} + \Delta u_x(x), \tag{2}$$

where

$$\Delta u_x = u_x^+ - u_x^-, \tag{3}$$

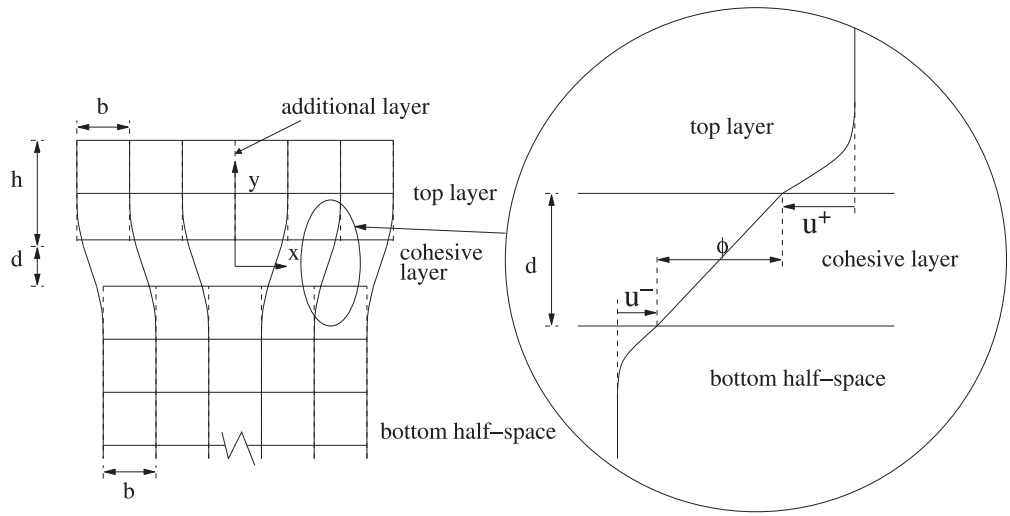

Figure 3. New half-space formed by joining top layer, bottom half-space and middle cohesive layer.

u_x^+ and u_x^- denote the displacements for the points above $y = 0$ and below $y = 0$, respectively. Similar to the PN model, the thickness of the cohesive layer cannot vanish for the HSPN model to be valid.

By isolating the free surface boundary effect, we split the displacement u_x into two components, u_x^∞ and u_x^b. The former denotes the displacement caused by the distributed dislocation in the unbounded domain, and the latter denotes the elastic displacements caused by the free surface. The disregistry at $y = 0$ is then given by

$$\phi_x(x) = \pm\frac{b}{2} + \Delta u_x^\infty(x) + \Delta u_x^b(x). \tag{4}$$

Note that, in the following, the superscripts ∞ and b are used to indicate that the components are induced by the dislocation at $y = 0$ in the unbounded domain and by the free surface at the boundary $y = h$, respectively.

We assume that the free surface boundary effect does not cause a discontinuous displacement field across the interface at $y = 0$, i.e. $\Delta u_x^b = 0$. The disregistry is then given by

$$\phi_x(x) = \pm\frac{b}{2} + \Delta u_x^\infty(x). \tag{5}$$

Hence, a classical relation between the Burgers vector density b' and Δu_x^∞ along the x-axis at $y = 0$ is recovered as

$$b'(x) = -\frac{\mathrm{d}\Delta u_x^\infty}{\mathrm{d}x}. \tag{6}$$

As noted in the previous study [7], the Burgers vector distribution can be viewed as an imposed eigen-strain that remains self-contained regardless of the existence of the free surface. The geometric core structure of the dislocation is therefore not related to the free surface. This assumption makes the HSPN model mathematically tractable, as shown in the following development.

2.2. Shear Stress Distribution

To obtain the shear stress σ_{xy} distribution in the half-space, the stress is separated again into two components as

$$\sigma_{xy} = \sigma^{\infty}_{xy} + \sigma^{b}_{xy} \tag{7}$$

and they will be solved separately. The stress σ^{∞}_{xy} at the glide plane by assuming that the traction-displacement relation still obeys the sinusoidal force law inside the glide plane (non-Hookean cohesive layer). The traction-free surface effect is removed as shown in the following:

$$\sigma^{\infty}_{xy}(x, 0) = -\tau_{\max} \sin \frac{2\pi \Delta u^{\infty}_{x}}{b}, \tag{8}$$

where

$$\tau_{\max} = \frac{\mu b}{2\pi d} \tag{9}$$

is chosen for the elastic limit to apply in small deformation theory. The following classical solutions [22] are then recovered:

$$\sigma^{\infty}_{xy}(x, 0) = \frac{\bar{\mu} b x}{x^2 + w_h^2}, \tag{10}$$

$$\Delta u^{\infty}_{x}(x, 0) = -\frac{b}{\pi} \tan^{-1} \frac{x}{w_h}, \tag{11}$$

and

$$b'(x) = \frac{b}{\pi} \frac{w_h}{x^2 + w_h^2}, \tag{12}$$

where $\bar{\mu} = \frac{\mu}{2\pi(1-\nu)}$ is the normalized shear modulus and $w_h = \frac{d}{2(1-\nu)}$ is the dislocation half width.

It is well known that the application of an image dislocation at $y = 2h$ with the opposite Burgers vector does not eliminate all the stress components on the free surface for an edge dislocation. This is also true for the HSPN model that has a distributed edge dislocation (see Figure 4 for how a distributed image dislocation may be applied).

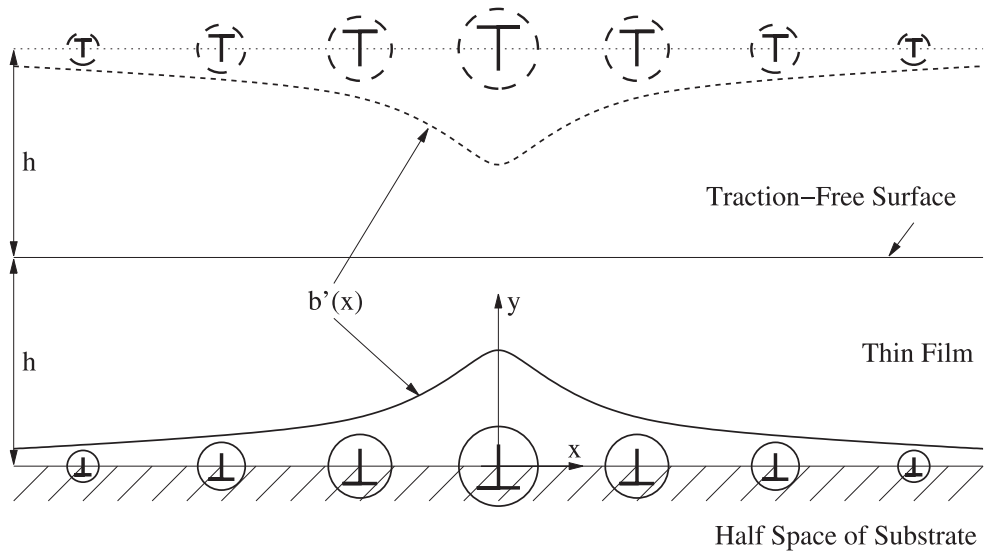

Figure 4. A distributed edge image dislocation at $y = 2h$ (outside the physical domain).

To obtain the stress σ^b_{xy} distribution for the HSPN model, the convolution theory can be applied on the Airy stress function for a single edge dislocation in a half-space. The Airy stress for a single edge dislocation in a half-space [23] is

$$\Phi(x, y) = -\bar{\mu} b \left\{ \frac{y}{2} \ln \left[\frac{x^2 + y^2}{x^2 + (y - 2h)^2} \right] - h \frac{x^2 + 2hy - y^2}{x^2 + (y - 2h)^2} \right\}, \quad y \le h. \tag{13}$$

This Airy stress function satisfies the Newtonian stress equilibrium and compatibility conditions, and the traction free boundary condition at $y = h$ under the plane strain conditions. This stress function can be split into three components as

$$\Phi(x, y) = \Phi^{\infty}(x, y) + \Phi^{I}(x, y) + \Phi^{3}(x, y) \tag{14}$$

where

$$\begin{aligned} \Phi^{\infty}(x, y) &= \frac{-\bar{\mu} b y}{2} \ln[x^2 + y^2], \\ \Phi^{I}(x, y) &= \frac{\bar{\mu} b (y - 2h)}{2} \ln[x^2 + (y - 2h)^2], \\ \Phi^{3}(x, y) &= \bar{\mu} b h \ln[x^2 + (y - 2h)^2] + \bar{\mu} b h \frac{x^2 + 2hy - y^2}{x^2 + (y - 2h)^2}. \end{aligned} \tag{15}$$

The stress function Φ^{∞} corresponds to the single edge dislocation at the origin in an infinite space, the stress function Φ^{I} corresponds to the single image edge dislocation at $y = 2h$ in an infinite space, and the stress function Φ^{3} corresponds to the additional component that ensures zero traction at $y = h$. These three stress functions combine to form the Airy stress function for an edge dislocation in a half-space with depth h. It confirms that the image dislocation itself is not sufficient to remove the traction at $y = h$ due to the edge dislocation at the origin. Therefore, the idea for constructing the HSPN model for the edge dislocation is different from that for the screw dislocation. The latter requires only the image dislocation [7]. For the edge dislocation, the HSPN model is better constructed using the Airy stress function in Equation (13).

With the use of convolution method and the Burgers vector given in Equation (12), the Airy stress function for the HSPN model can be expressed as

$$\Phi_{\mathrm{HSPN}}(x, y) = \int_{-\infty}^{\infty} b'(x - x') \frac{\Phi(x', y)}{b} \, \mathrm{d}x' \tag{16}$$

To solve for Equation (16), the residue theorem [24] is used to obtain the Airy stress function of the HSPN model for an edge dislocation, given by

$$\begin{aligned} \Phi_{\mathrm{HSPN}}(x, y) &= -\bar{\mu} b \left\{ \frac{y}{2} \ln \left[\frac{x^2 + (|y| + w_h)^2}{x^2 + (y - m)^2} \right] - h \left[1 - \frac{2(y - h)(y - m)}{x^2 + (y - m)^2} \right] \right\}, \\ & \quad y \leq h \end{aligned} \tag{17}$$

where $m = 2h + w_h$. Since the original Airy stress function in Equation (13) satisfies the Newtonian stress equilibrium conditions, the obtained Airy stress function in Equation (17) for the HSPN model of edge dislocations also satisfies the Newtonian stress equilibrium conditions.

To isolate the boundary effect at the free surface, the stress function is split into two components:

$$\Phi_{\mathrm{HSPN}}(x, y) = \Phi^{\infty}_{\mathrm{HSPN}}(x, y) + \Phi^{b}_{\mathrm{HSPN}}(x, y) \tag{18}$$

where

$$\begin{aligned} \Phi^{\infty}_{\mathrm{HSPN}}(x, y) &= -\frac{\bar{\mu} b y}{2} \ln[x^2 + (|y| + w_h)^2], \\ \Phi^{b}_{\mathrm{HSPN}}(x, y) &= \bar{\mu} b \left\{ \frac{y}{2} \ln[x^2 + (y - m)^2] + h \left[1 - \frac{2(y - h)(y - m)}{x^2 + (y - m)^2} \right] \right\} \end{aligned} \tag{19}$$

In the following development, the subscript HSPN is omitted for simplicity.

Taking the partial derivative of the Airy stress function $\Phi^{b}_{\mathrm{HSPN}}(x, y)$ with respect to x and y gives the boundary component of the shear stress distribution as

$$\sigma^{b}_{xy}(x,y) = \bar{\mu}b\left\{\frac{-x}{x^2+(y-m)^2} + \frac{2x(y-2h)(y-m)-2hx(y-h)}{[x^2+(y-m)^2]^2} + \frac{16hx(y-h)(y-m)^2}{[x^2+(y-m)^2]^3}\right\} \tag{20}$$

The shear stress distribution at the dislocation ($y = 0$) due to the boundary condition is then given by

$$\sigma^{b}_{xy}(x,0) = \bar{\mu}b\left\{\frac{-x}{x^2+m^2} + \frac{4h(h+m)x}{(x^2+m^2)^2} - \frac{16h^2m^2x}{(x^2+m^2)^3}\right\}. \tag{21}$$

3. MODIFIED MISFIT ENERGY AND PEIERLS STRESS

In the HSPN model, in addition to the stress due to the dislocation, the stress at the glide plane due to the free surface also interacts with the dislocation. Thus, the formulas for calculating the misfit energy and the Peierls stress in the half-space should be modified considering σ^{b}_{xy} shown in Equation (21).

3.1. Misfit Energy

To calculate the misfit energy, we adopt the discrete summation procedure used in [7, 8]. This approach is physically realistic since the resulting misfit energy has the correct period. This is especially important for narrow dislocations ($d \ll s$), where s is the lattice spacing, and the resulting Peierls stress also fits well to the atomistic theory.

3.1.1. Misfit energy density

The misfit energy can be obtained by summing the misfit energy density over the glide plane. The local misfit shear strain at the glide plane of the dislocation is

$$\gamma_{xy}(x,0) = \frac{\phi_x}{d} = \pm\frac{b}{2d} + \frac{\Delta u^{\infty}_{x}}{d}. \tag{22}$$

The misfit energy density, which is the unit misfit energy stored in a volume element of height d, lattice spacing s, unit depth in the z-direction and at the glide plane ($y = 0$), can then be written as

$$\begin{aligned}\Delta W(x) &= sd\int_0^{\gamma_{xy}} \sigma_{xy}(x,0)\mathrm{d}\gamma_{xy} \\ &= s\int_{\mp b/2}^{\Delta u^{\infty}_{x}} \sigma^{\infty}_{xy}(x,0)\mathrm{d}\Delta u^{\infty}_{x} + s\int_{\mp b/2}^{\Delta u^{\infty}_{x}} \sigma^{b}_{xy}(x,0)\mathrm{d}\Delta u^{\infty}_{x}.\end{aligned} \tag{23}$$

This misfit energy density is stored between a pair of atomic planes separated by a distance s. For comparison, the misfit energy density is split into ΔW^{∞}, the conventional misfit energy density, and ΔW^{b}, the misfit energy due to the boundary condition. The conventional misfit energy density can be calculated as

$$\Delta W^{\infty}(x) = s\int_{\mp b/2}^{\Delta u_x^{\infty}} \sigma_{xy}^{\infty}(x,0)\mathrm{d}\Delta u_x^{\infty} = \frac{sW_o}{2\pi w_h}\left(\cos\frac{2\pi\Delta u_x^{\infty}}{b}+1\right) \tag{24}$$

where $W_o = \bar{\mu}b^2/2$.

For the boundary component, the stress is split into three components as

$$\sigma_{xy}^{b}(x,0) = \sigma_{xy}^{b1}(x,0) + \sigma_{xy}^{b2}(x,0) + \sigma_{xy}^{b3}(x,0) \tag{25}$$

where

$$\begin{aligned}
\sigma_{xy}^{b1}(x,0) &= -\frac{\bar{\mu}x}{x^2+m^2}\\
\sigma_{xy}^{b2}(x,0) &= \frac{4\bar{\mu}xh(h+m)}{(x^2+m^2)^2}\\
\sigma_{xy}^{b3}(x,0) &= -\frac{16\bar{\mu}xh^2m^2}{(x^2+m^2)^3}
\end{aligned} \tag{26}$$

and similarly the misfit energy density due to the boundary condition is

$$\Delta W^{b} = \Delta W^{b1} + \Delta W^{b2} + \Delta W^{b3} \tag{27}$$

where

$$\Delta W^{bi} = s\int_{\mp b/2}^{\Delta u_x^{\infty}} \sigma_{xy}^{bi}(x,0)\mathrm{d}\Delta u_x^{\infty}, \quad i=1,2,3. \tag{28}$$

Following integration of the expression shown in Equation (28) and simplification, we obtain

$$\begin{aligned}
\Delta W^{b1} &= -\frac{W_o\kappa}{\rho}\ln\left[\frac{x^2+m^2}{x^2+w_h^2}\right]\\
\Delta W^{b2} &= \frac{W_o\kappa(h+m)}{\rho(h+w_h)}\left\{\ln\left[\frac{x^2+m^2}{x^2+w_h^2}\right] - \frac{4h(h+w_h)}{x^2+m^2}\right\}\\
\Delta W^{b3} &= \frac{W_o\kappa m^2}{\rho(h+w_h)^2}\left\{\ln\frac{x^2+w_h^2}{x^2+m^2} + \frac{(m^2-w_h^2)}{x^2+m^2} + \frac{(m^2-w_h^2)^2}{2(x^2+m^2)^2}\right\}
\end{aligned} \tag{29}$$

where κ and ρ are two dimensionless parameters that depend on the thickness h and are defined as

$$\rho(h) = \frac{4\pi h}{s}, \quad \kappa(h) = \frac{w_h}{h + w_h}. \tag{30}$$

By grouping the similar terms in Equation (29), ΔW^b may also be expressed as

$$\begin{aligned} \Delta W^b &= \Delta W^{bI} + \Delta W^{bII} + \Delta W^{bIII} \\ &= -AW_o \ln\left[\frac{x^2 + m^2}{x^2 + w_h^2}\right] + BW_o \frac{s^2\beta^2}{2\pi^2(x^2 + m^2)} + CW_o \frac{s^4\beta^3}{4\pi^4(x^2 + m^2)^2} \end{aligned} \tag{31}$$

where

$$A = \frac{\kappa}{\rho}(1 + (1 - \kappa)^2), \quad B = \frac{\kappa\rho}{2\beta}(1 - \kappa), \quad C = \frac{\kappa\rho}{2\beta} \tag{32}$$

are the three dimensionless coefficients and $\beta = 2\pi m/s$.

3.1.2. Total misfit energy

The total misfit energy will be formulated as a function of the position of the dislocation since it leads to the calculation of the Peierls stress directly. When the origin of the dislocation is introduced at the position $x = a$, $0 < a < s$, the atomic planes at ks, where $k = 0, \pm 1, \pm 2, \ldots$, will experience a relative displacement $\Delta u_x^{\infty}(ks - a)$, with the dislocation core structure remains the same during the translation, i.e. rigid translation [6]. Therefore, to calculate the total misfit energy in the lattice, the argument x of the misfit energy density in Equation (23) is replaced by $ks - a$ and the misfit energy density is summed along the glide plane over the lattice (over k), as

$$W(a) = \sum_{k=-\infty}^{\infty} \Delta\tilde{W}(k, a), \tag{33}$$

where the symbol tilde ($\tilde{}$) indicates that the energy W takes the arguments k and a instead of x. Similarly, the total misfit energy is split into two parts, $W^{\infty}(a)$ and $W^b(a)$, in order to compare with the PN model. The former is the misfit energy due to $\Delta\tilde{W}^{\infty}$, i.e.

$$\hat{W}^{\infty}(\alpha) = \sum_{k=-\infty}^{\infty} \Delta\tilde{W}^{\infty}(k, a). \tag{34}$$

The symbol hat ($\hat{}$) indicates that the energy W^{∞} takes the argument α instead of a. By utilizing the Poisson's summation formula in the harmonic analysis we can rewrite Equation (34) as

$$\hat{W}^{\infty}(\alpha) = \sum_{k=-\infty}^{\infty} \Delta\tilde{W}^{\infty}(k, a) = \sum_{j=-\infty}^{\infty} \int_{-\infty}^{\infty} \Delta\tilde{W}^{\infty}(t, a) \mathrm{e}^{-\mathrm{i}2\pi tj}\, \mathrm{d}t. \tag{35}$$

By solving the integral in Equation (35) we have

$$\hat{W}^{\infty}(\alpha) = W_o \left[1 + 2 \sum_{j=1}^{\infty} \mathrm{e}^{-\xi j} \cos(j\alpha) \right], \tag{36}$$

where $\xi = 2\pi w_h/s$, $\alpha = 2\pi a/s$ are the two normalized dimensionless quantities. By expressing the cosine function in terms of exponentials, the geometric series in Equation (34) can be summed [8] to yield

$$\hat{W}^{\infty}(\alpha) = W_o \frac{\sinh \xi}{\cosh \xi - \cos \alpha}. \tag{37}$$

For W^b due to $\Delta\tilde{W}^b$, we have three terms (see Equation (31)). To determine the total misfit energy, the Poisson summation formula in the harmonic analysis is utilized again such that

$$\begin{aligned}
\hat{W}^{bI}(\alpha) &= \sum_{k=-\infty}^{\infty} \Delta\tilde{W}^{bI}(k,a) = \sum_{j=-\infty}^{\infty} \int_{-\infty}^{\infty} \Delta\tilde{W}^{bI}(t,a) \mathrm{e}^{-\mathrm{i}2\pi tj}\, \mathrm{d}t, \\
\hat{W}^{bII}(\alpha) &= \sum_{k=-\infty}^{\infty} \Delta\tilde{W}^{bII}(k,a) = \sum_{j=-\infty}^{\infty} \int_{-\infty}^{\infty} \Delta\tilde{W}^{bII}(t,a) \mathrm{e}^{-\mathrm{i}2\pi tj}\, \mathrm{d}t, \\
\hat{W}^{bIII}(\alpha) &= \sum_{k=-\infty}^{\infty} \Delta\tilde{W}^{bIII}(k,a) = \sum_{j=-\infty}^{\infty} \int_{-\infty}^{\infty} \Delta\tilde{W}^{bIII}(t,a) \mathrm{e}^{-\mathrm{i}2\pi tj}\, \mathrm{d}t.
\end{aligned} \tag{38}$$

By solving the integrals in Equation (38) we have

$$\begin{aligned}
\hat{W}^{bI}(\alpha) &= -AW_o \left[\rho + 2 \sum_{j=1}^{\infty} \frac{1}{j} \mathrm{e}^{-\xi j} \left(1 - \mathrm{e}^{-\rho j}\right) \cos(\alpha j) \right], \\
\hat{W}^{bII}(\alpha) &= BW_o \left[1 + 2 \sum_{j=1}^{\infty} \mathrm{e}^{-\beta j} \cos(\alpha j) \right], \\
\hat{W}^{bIII}(\alpha) &= CW_o \left[1 + 2 \sum_{j=1}^{\infty} (1 + \beta j) \mathrm{e}^{-\beta j} \cos(\alpha j) \right].
\end{aligned} \tag{39}$$

The above expressions include a Mercator series, a geometric series, and a series that has the following form in each jth term

$$j a^j \cos(bj), \quad |a| < 1. \tag{40}$$

All these series have closed-form solutions when they are summed up (see [25] for the series shown in Equation (40)). Therefore, Equation (39) becomes

$$\begin{aligned}
\hat{W}^{bI}(\alpha) &= -AW_o \ln\left[\frac{\cosh\beta - \cos\alpha}{\cosh\xi - \cos\alpha}\right], \\
\hat{W}^{bII}(\alpha) &= BW_o \frac{\sinh\beta}{\cosh\beta - \cos\alpha}, \\
\hat{W}^{bIII}(\alpha) &= CW_o\left[\frac{\sinh\beta}{\cosh\beta - \cos\alpha} + \beta\frac{\cosh\beta\cos\alpha - 1}{(\cosh\beta - \cos\alpha)^2}\right].
\end{aligned} \tag{41}$$

When the size of the dislocation core is much smaller than the lattice constant (size), i.e. $\xi \ll 1$, the dislocation is categorized as a *narrow dislocation*. This implies that the constant term ($j = 0$) in the sum of Equation (33) contributes to the misfit energy most significantly, i.e.

$$W(a) \simeq \Delta\tilde{W}(0, a) \tag{42}$$

Hence, the four components of the total misfit energy for narrow dislocations are

$$\begin{aligned}
\hat{W}^{n,\infty}(\alpha) &= W_o \frac{2\xi}{\alpha^2 + \xi^2}, \\
\hat{W}^{n,bI}(\alpha) &= -AW_o \ln\left[\frac{\alpha^2 + \beta^2}{\alpha^2 + \xi^2}\right], \\
\hat{W}^{n,bII}(\alpha) &= BW_o \frac{2\beta}{\alpha^2 + \beta^2}, \\
\hat{W}^{n,bIII}(\alpha) &= CW_o \frac{4\beta^3}{(\alpha^2 + \beta^2)^2},
\end{aligned} \tag{43}$$

where the superscript n indicates that the quantity is for narrow dislocations.

When the size of the dislocation core is much bigger than the lattice constant (size), i.e. $\xi \gg 1$, the dislocation is categorized as a *wide dislocation*. Only the constant term ($j = 0$) and the leading term ($j = 1$) in the sum of Equations (34) and (39) contributes to the misfit energy significantly. Thus the four components of the total misfit energy for wide dislocations are

$$\begin{aligned}
\hat{W}^{w,\infty}(\alpha) &= W_o\left[1 + 2\mathrm{e}^{-\xi}\cos\alpha\right], \\
\hat{W}^{w,bI}(\alpha) &= -AW_o\left[\rho + 2\mathrm{e}^{-\xi}\left(1 - \mathrm{e}^{-\rho}\right)\cos\alpha\right], \\
\hat{W}^{w,bII}(\alpha) &= BW_o\left[1 + 2\mathrm{e}^{-\beta}\cos\alpha\right], \\
\hat{W}^{w,bIII}(\alpha) &= CW_o\left[1 + 2(1+\beta)\mathrm{e}^{-\beta}\cos\alpha\right],
\end{aligned} \tag{44}$$

where the superscript w indicates that the quantity is for wide dislocations.

3.2. Peierls Stress

The lattice friction σ due to W when the dislocation moves by a distance a is defined as

$$\sigma(a) = -\frac{1}{b}\frac{\mathrm{d}W(a)}{\mathrm{d}a} \tag{45}$$

or

$$\hat{\sigma}(\alpha) = -\frac{2\pi}{bs}\frac{\mathrm{d}\hat{W}(\alpha)}{\mathrm{d}\alpha} \tag{46}$$

when the argument is α. The Peierls stress, which is the minimum external stress required to move the dislocation irreversibly, is then given as the maximum of the lattice friction

$$\sigma_p = \max_{\alpha} \hat{\sigma}(\alpha) = \hat{\sigma}(\alpha_m) \tag{47}$$

where α_m is the maximizer.

The four components of the Peierls stress for the edge dislocation in the half-space may then be expressed as

$$\begin{aligned}
\sigma_p^{\infty} &= \sigma_o \frac{\sinh\xi \sin\alpha_m}{2(\cosh\xi - \cos\alpha_m)^2}, \\
\sigma_p^{bI} &= -A\sigma_o \frac{(\cosh\beta - \cosh\xi)\sin\alpha_m}{2(\cosh\xi - \cos\alpha_m)(\cosh\beta - \cosh\alpha_m)}, \\
\sigma_p^{bII} &= B\sigma_o \frac{\sinh\beta \sin\alpha_m}{2(\cosh\beta - \cos\alpha_m)^2}, \\
\sigma_p^{bIII} &= C\sigma_o \frac{(\cosh\xi\cosh\beta + \cosh\xi\cos\alpha_m - 2)\sin\alpha_m}{2(\cosh\beta - \cos\alpha_m)^3},
\end{aligned} \tag{48}$$

where $\sigma_o = \frac{\mu b}{s(1-\nu)}$. For narrow dislocations, the four components of the Peierls stress are

$$\begin{aligned}
\sigma_p^{n,\infty} &= \sigma_o \frac{2\xi\alpha_m^n}{[(\alpha_m^n)^2 + \xi^2]^2}, \\
\sigma_p^{n,bI} &= -A\sigma_o \frac{(\beta^2 - \xi^2)\alpha_m^n}{[(\alpha_m^n)^2 + \xi^2][(\alpha_m^n)^2 + \beta^2]}, \\
\sigma_p^{n,bII} &= B\sigma_o \frac{2\beta\alpha_m^n}{[(\alpha_m^n)^2 + \beta^2]^2}, \\
\sigma_p^{n,bIII} &= C\sigma_o \frac{8\beta^3\alpha_m^n}{[(\alpha_m^n)^2 + \beta^2]^3},
\end{aligned} \tag{49}$$

where α_m^n is the maximizer for narrow dislocations. For wide dislocations, where $\alpha_m^w = \pi/2$, the four components of the Peierls stress are

$$\begin{aligned}
\sigma_p^{w,\infty} &= \sigma_o e^{-\xi}, \\
\sigma_p^{w,bI} &= -A\sigma_o e^{-\xi}(1 - e^{-\rho}), \\
\sigma_p^{w,bII} &= B\sigma_o e^{-\beta}, \\
\sigma_p^{w,bIII} &= C\sigma_o(1+\beta)e^{-\beta}.
\end{aligned} \tag{50}$$

4. SCALING FACTORS

To study the effect of the free surface on both misfit energy and Peierls stress of the edge dislocation in the half-space, the scaling factor f is introduced [7] (it was called the *amplification factor* in [7]). The scaling factor f, which will be a function of the depth h of the dislocation, is defined as the ratio between the HSPN solutions and the conventional PN solutions. It provides a scaling law on how the misfit energy and the Peierls stress change with varying depth from the free surface. The expression for f will be given for dislocations of general sizes and for the special cases of narrow and wide dislocations. Emphasis will be placed on the asymptotic behavior of this factor as the depth h approaches its minimum $h_{\min}$.

As noted earlier, the HSPN model requires a non-vanishing non-Hookean slab joining the top layer and the bottom half-space. The depth h for the HSPN model therefore cannot vanish. The minimum depth for the model to be valid is $d/2$, i.e. $h_{\min} = d/2$. The dislocation that corresponds to the minimum depth $h_{\min}$ is then understood as a surface dislocation.

4.1. Misfit Energy

In this paper, the scaling factor for the misfit energy is defined as the ratio of the maximum misfit energies, i.e.

$$f_W(h) \equiv \frac{W_{\max}}{W_{\max}^{\infty}} \tag{51}$$

The misfit energies of the Peierls dislocation are periodic functions that have maximum values when the dislocation is in the unshifted position, i.e. $\alpha = 0$. Hence, the scaling factor for dislocations is

$$f_W(h) = 1 + \frac{\cosh\xi - 1}{\sinh\xi}\left\{-A\ln\left[\frac{\cosh\beta - 1}{\cosh\xi - 1}\right] + \frac{(B+C)\sinh\beta + C\beta}{\cosh\beta - 1}\right\}. \tag{52}$$

For narrow dislocations, the scaling factor is

$$f_W^n(h) = 1 + \xi \left\{ -A \ln \left[\frac{\beta}{\xi} \right] + \frac{1}{\beta}(B + 2C) \right\}. \tag{53}$$

For wide dislocations, the scaling factor is

$$f_W^w(h) = 1 + \frac{-A\rho + B + C}{1 + 2e^{-\xi}} + \frac{2e^{-\xi}}{1 + 2e^{-\xi}} \{ e^{-\rho}[A + B + C(1 + \beta)] - A \}. \tag{54}$$

The above factor can also be approximated as

$$f_W^w(h) \simeq 1 - A\rho + B + C, \tag{55}$$

since $e^{-\xi} \to 0$ for increasing w_h.

We define

$$f_{W,\min} \equiv f_W(h_{\min}) \tag{56}$$

to be the scaling factor for surface dislocations. Then, the scaling factor $f_{W,\min}$ for narrow dislocations is given by

$$f_{W,\min}^n = 1 - \frac{(1-\nu)^2 + (2-\nu)^2}{2(1-\nu)(2-\nu)^3} \ln(3 - 2\nu) + \frac{(1-\nu)(5-3\nu)}{(2-\nu)^2(3-2\nu)^2}, \tag{57}$$

and for wide dislocations is given by

$$f_{W,\min}^w = 1 - \frac{1}{(2-\nu)} + \frac{(1-\nu)}{(2-\nu)^2} - \frac{(1-\nu)^2}{(2-\nu)^3}. \tag{58}$$

The above two equations show that the scaling factors $f_{W,\min}^n$ and $f_{W,\min}^w$ for surface dislocations are dependent on the Poisson's ratio ν alone. However, as discussed subsequently, the scaling factors $f_{W,\min}$ for surface dislocations of general sizes also depend on ξ.

4.2. Peierls Stress

The scaling factor for the Peierls stress is defined as

$$f_\sigma(h) \equiv \frac{\sigma_p}{\hat{\sigma}^\infty(\alpha_m^\infty)}, \tag{59}$$

where $\hat{\sigma}^\infty(\alpha_m^\infty)$ is the Peierls stress for the edge dislocation in bulk materials. The maximizer α_m^∞ is given by

$$\alpha_m^\infty = \cos^{-1}\left(\frac{1}{2} \left(\sqrt{9 + \sinh^2 \xi} - \cosh \xi \right) \right) \tag{60}$$

for dislocations of all sizes [8]. The value of α_m^∞ is $\xi/\sqrt{3}$ and $\pi/2$ for narrow dislocations and wide dislocations, respectively.

From Equations (48) and (49), the closed-form expression for α_m and α_m^n may not be readily obtained. Therefore, the scaling factors for both dislocations of all sizes and narrow dislocations will not be given explicitly. If necessary, they can be calculated from Equations (48) and (49) numerically by using Newton's method [24].

For wide dislocations, the maximizer α_m^w is $\pi/2$. Hence, the scaling factor for wide dislocations is

$$f_\sigma^w(h) = (1 - A) + \mathrm{e}^{-\rho}[A + B + C(1 + \beta)]. \tag{61}$$

The above factor can also be approximated as

$$f_W^w(h) \simeq 1 - A, \tag{62}$$

since $\mathrm{e}^{-\rho} \to 0$ for increasing w_h.

The scaling factor for surface dislocations is defined as

$$f_{\sigma,\min} \equiv f_\sigma(h_{\min}). \tag{63}$$

In the case of wide dislocations, it may be expressed as

$$f_{\sigma,\min}^w = 1 - \frac{(1-\nu)^2 + (2-\nu)^2}{2(1-\nu)(2-\nu)^3\xi}. \tag{64}$$

The above equation shows that $f_{\sigma,\min}^w$ is dependent on the Poisson ratio ν and the size of the dislocation ξ. Even though the expression of the scaling factor of surface dislocations for narrow dislocations, $f_{\sigma,\min}^n$, is not shown here, a numerical study has been done and $f_{\sigma,\min}^n$ is found to be only dependent on the Poisson ratio.

To show how the misfit energy and the Peierls stress change with the depth of the dislocation, the scaling factors f_W and f_σ are plotted versus the normalized thickness h/s for different core size d/s ratios in Figure 5. A Poisson ratio of $\nu = 0.3$ is selected for the purposes of illustration. In these two plots, the middle five curves (three with a marker "$\circ$", and two with solid lines and markers "$\triangle$" or "$\triangledown$") are plotted by using the exact scaling factors shown in Equations (48) and (52).

For comparison, we also use the approximated scaling factors shown in Equations (53) and (55), and Equations (49) and (62) to plot the other two curves for both narrow ($d/s = 0.25$) and wide ($d/s = 4$) dislocations, respectively.

From Figure 5a, the free surface effect on the misfit energy is shown to be quite significant. For the dislocation with the core size $d/s = 1$, the reduction in the maximum misfit energy can be as high as about 45% for a surface dislocation. In general, the reduction becomes less than 5% only when the dislocation is at least 50 layers of atoms away ($h/s > 50$) from the free surface. The effect of the free surface is larger on wide dislocations than on narrow dislocations. It is also true for surface dislocations, where the reduction in the misfit energy is about 45% for wide dislocations and is about 30% for narrow dislocations. The scaling factors for the surface dislocations of general sizes depend on the core sizes, and thus

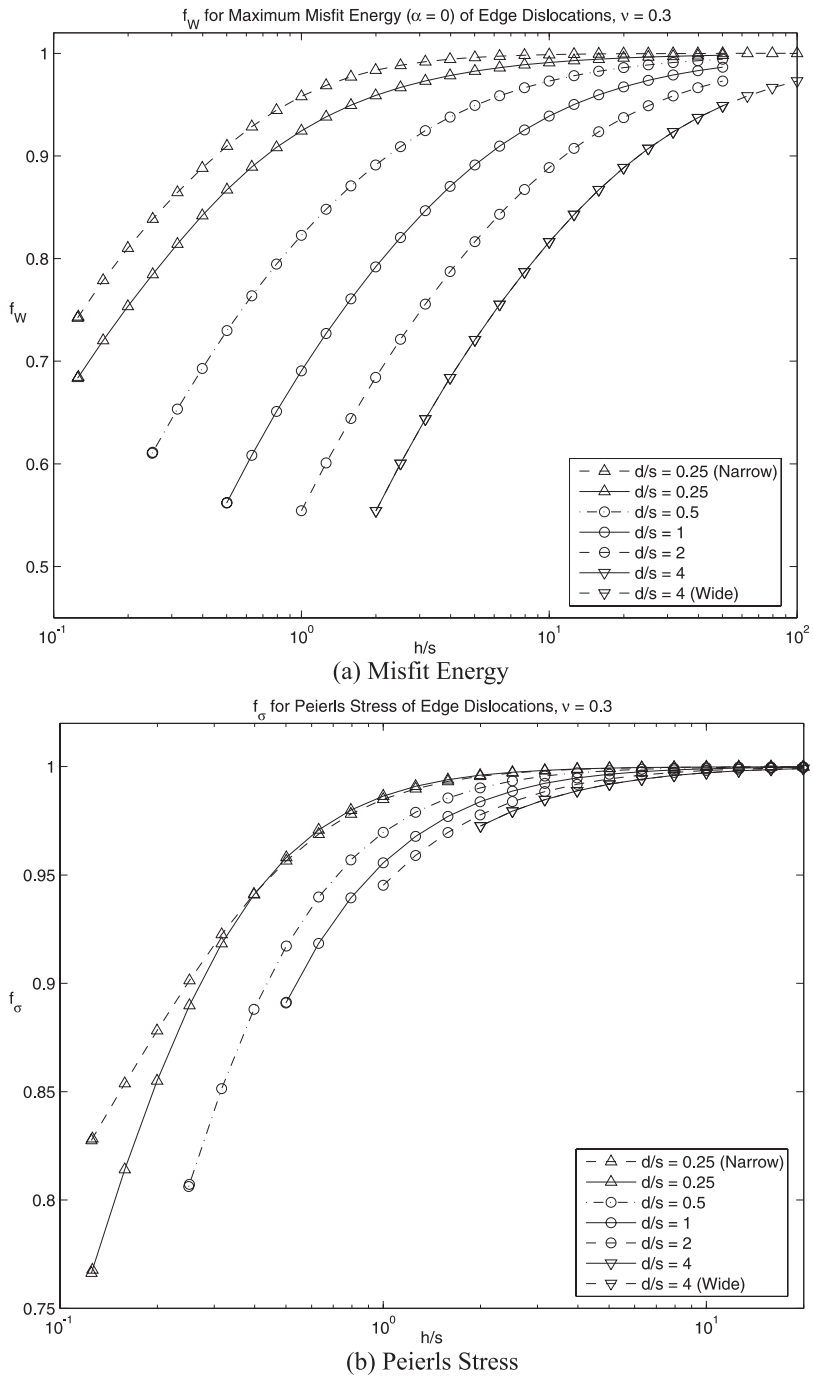

Figure 5. Scaling factors versus h/s for different d/s ratios.

on the parameter ξ of the dislocations. Also, for narrow dislocations, the reduction is already less than 5% when at least one layer of atoms is on top of the dislocation.

For the estimate of the scaling factors, the formula in Equation (55) approximates the exact scaling factor very accurately for wide dislocations. For narrow dislocations, however, the approximated scaling factor given in Equation (53) does not fit the exact curve quite well. Therefore, the formula of the scaling factor for narrow dislocations should be good only when the core size d/s is much less than 0.25.

Compared with the effect on the misfit energy, the free surface effect on the Peierls stress of the dislocation is not as significant (see Figure 5b). The effect of the free surface is also larger on wide dislocations than on narrow dislocations. For surface dislocations, however, the reduction is less for wide dislocations than for narrow dislocations. The reduction in the Peierls stress is about 5% for wide dislocations and is about 24% for narrow dislocations. For the dislocation with the core size $d/s = 1$, the reduction in the Peierls stress does not exceed 11%. When at least one layer of atoms is above the dislocation, i.e. $h/s = 1.5$, the reduction becomes less than 5%.

The expression for the scaling factor obtained from Equation (49) for narrow dislocations and for wide dislocations obtained from Equation (62) are shown to approximate the exact scaling factors very accurately. For narrow dislocations, the approximated curve only starts deviating from the true curve when the depth of the dislocation is much smaller than two to three times the core size.

The above observations are also found in the results for the screw dislocations discussed in [7]. Therefore, the scaling factors for edge dislocations have similar properties to those for screw dislocations, with the important exception that the former are dependent on the Poisson ratio while the latter are not.

5. CONCLUSIONS

The half-space Peierls–Nabarro (HSPN) model recently proposed in [7] has been successfully extended to the case of edge dislocations. Similar to the case of screw dislocations, the Burgers vector is also distributed with the same displacement profile as that in the Peierls–Nabarro model. With this model, the closed-form expressions for both the misfit energy and Peierls stress have been obtained for an edge dislocation in a half-space. These expressions allow us to study the free surface effect on the misfit energy and the Peierls stress. Since analytical formulas can be obtained from the HSPN model, it is possible that this model may serve as a good approximation of atomistic simulations for crystal structures with a free-surface boundary.

By comparing the HSPN model to the conventional PN model, we have derived the scaling factors for edge dislocations of general sizes as well as for the two limiting cases: narrow and wide dislocations. The scaling factors have provided scaling laws for both the misfit energy and Peierls stress and for different depths of the dislocations in the half-space. Emphasis has also been put on the scaling factors for the surface dislocations.

The scaling factors for the edge dislocation have similar properties to those for the screw dislocation except that the former are dependent on the Poisson ratio. The reduction due to

the free surface effect for the misfit energy can be as high as 45% for a surface dislocation. This effect becomes less significant only when the dislocation is more than 50 layers of atoms away from the free surface. On the contrary, the free surface effect on the Peierls stress is much less significant. For the Poisson ratio $\nu = 0.3$, the reduction in the Peierls stress does not exceed 25%.

REFERENCES

[1] Vendik, O. G., Zubko, S. P. and Ter-martirosayn, L. T. Experimental evidence of the size effect in thin ferroelectric films. *Applied Physics Letters,* 73, 37–39 (1998).

[2] Espinosa, H. and Prorok, B. Size effects on the mechanical behavior of gold thin films. *Journal of Materials Science,* 38, 4125–4128 (2003).

[3] Bazant, Z., Guo, Z., Espinosa, H., Zhu, Y. and Peng, B. Epitaxially influenced boundary layer model for size effect in thin metallic films. *Journal of Applied Physics,* 97, 073506 (2005).

[4] Han, C.-S., Hartmaiera, A., Gao, H. and Huang, Y. Discrete dislocation dynamics simulations of surface induced size effects in plasticity. *Materials Science and Engineering: A,* 415, 225–233 (2005).

[5] Peierls, R. The size of a dislocation. *Proceedings of the Physical Society of London,* 52, 34–37 (1940).

[6] Nabarro, F. R. N. Dislocations in a simple cubic lattice. *Proceedings of the Physical Society of London,* 59, 256–272 (1947).

[7] Lee, C.-L. and Li, S. A half-space Peierls–Nabarro model and the mobility of screw dislocations in a thin film. *Acta Materialia,* 55, 2149–2157 (2007).

[8] Joos, B. and Duesbery, M. S. The Peierls stress of dislocations: An analytic formula. *Physical Review Letters,* 78, 266–269 (1997).

[9] Vitek, V. Intrinsic stacking faults in body-centred cubic crystals. *Philosophical Magazine,* 18, 773–786 (1968).

[10] Joos, B., Ren, Q. and Duesbery, M. S. Peierls–Nabarro model of dislocations in silicon with generalized stacking-fault restoring forces. *Physical Review B,* 50, 5890–5898 (1994).

[11] Schoeck, G. The generalized Peierls–Nabarro model. *Philosophical Magazine A—Physics of Condensed Matter Structure Defects and Mechanical Properties,* 69, 1085–1095 (1994).

[12] Juan, Y. M. and Kaxiras, E. Generalized stacking fault energy surfaces and dislocation properties of silicon: A first-principles theoretical study. *Philosophical Magazine A—Physics of Condensed Matter Structure Defects and Mechanical Properties,* 74, 1367–1384 (1996).

[13] Bulatov, V. V. and Kaxiras, E. Semidiscrete variational Peierls framework for dislocation core properties. *Physical Review Letters,* 78, 4221–4224 (1997).

[14] Hartford, J., von Sydow, B., Wahnstrom, G. and Lundqvist, B. I. Peierls barriers and stresses for edge dislocations in Pd and Al calculated from first principles. *Physical Review B,* 58, 2487–2496 (1998).

[15] G. Schoeck, The Peierls energy revisited. *Philosophical Magazine a-Physics of Condensed Matter Structure Defects and Mechanical Properties,* 79 (11) (1999) 2629–2636.

[16] Schoeck, G. Peierls energy of dislocations: A critical assessment. *Physical Review Letters,* 82, 2310–2313 (1999).

[17] Wang, J. N. A new modification of the formulation of Peierls stress, *Acta Materialia,* 44, 1541–1546 (1996).

[18] Wang, J. N. Prediction of Peierls stresses for different crystals. *Materials Science and Engineering A—Structural Materials Properties Microstructure and Processing,* 206, 259–269 (1996).

[19] Lu, G., Kioussis, N., Bulatov, V. and Kaxiras, E. The Peierls–Nabarro model revisited. *Philosophical Magazine Letters,* 80, 675–682 (2000).

[20] Nabarro, F. R. N. Fifty-year study of the Peierls–Nabarro stress. *Materials Science and Engineering A—Structural Materials Properties Microstructure and Processing,* 234, 67–76 (1997).

[21] Schoeck, G. The Peierls model: Progress and limitations. *Materials Science and Engineering A—Structural Materials Properties Microstructure and Processing,* 400, 7–17 (2005).

[22] Hirth, J. P. and Lothe, J. *Theory of Dislocations,* 2nd Edition, Krieger, Malabar, FL, 1992.

[23] Freund, L. B. and Suresh, S. *Thin Film Materials: Stress, Defect Formation, and Surface Evolution,* Cambridge University Press, New York, 2003.

[24] Kreyszig, E. *Advanced Engineering Mathematics,* Wiley, New York, 8th edition, 1998.

[25] Hansen, E. R. *A Table of Series and Products,* Prentice-Hall Series in Automatic Computation, Prentice-Hall, Englewood Cliffs, NJ, 1975.